International Journal of Nanomedicine

Dovepress

open access to scientific and medical research

Open Access Full Text Article

ORIGINAL RESEARCH

Hydroxyl Group-Targeted Conjugate and Its Self-Assembled Nanoparticle of Peptide Drug: Effect of Degree of Saturation of Fatty Acids and Modification of Physicochemical Properties

Jisoo Park[1,*], Hai V Ngo[1,*], Hyo-Eon Jin[1], Kye Wan Lee[2], Beom-Jin Lee[1]

[1]Bioavailability Control Laboratory, College of Pharmacy, Ajou University, Suwon, 16499, Republic of Korea; [2]Dongkook Pharmaceutical Co., Ltd, Seoul, Republic of Korea

*These authors contributed equally to this work

Correspondence: Beom-Jin Lee, Bioavailability Control Laboratory, College of Pharmacy, Ajou University, Suwon, 16499, Republic of Korea, Tel +82 312193442, Fax +82 312193435, Email bjl@ajou.ac.kr

Purpose: To conjugate different degree of saturation of C18 fatty acids (stearic acid, oleic acid, and linoleic acid) with the hydroxyl groups of leuprolide acetate (LEU acetate) and to investigate the controlled release and enhanced permeability through self-assembled nanoparticles (L18FNs).

Methods: Yamaguchi esterification with benzoyl chloride and DMAP (4-Dimethylaminopyridine) allowed the conjugation of the fatty acid to the hydroxyl group of LEU. The three conjugates were then designated as stearic acid-conjugated LEU, LSC, oleic acid-conjugated LEU, LOC, and linoleic acid-conjugated LEU, LLC, respectively. The conjugates (L18FCs) were purified using preparative HPLC (Prep-HPLC) and identified through various instrumental analyses.

Results: The zeta potential, particle size, and morphology of each L18FNs were evaluated. In the case of LSNs, the zeta potential value was relatively low and the particle size was larger than LONs and LLNs owing to the higher hydrophobicity of saturated fatty chain, while the LLNs showed a higher zeta potential and smaller particle size. In human plasma, LLC showed the fastest degradation rate with the highest accumulative drug release. The permeability of L18FNs was analyzed through the Franz diffusion cell experiment, confirming that the degree of saturation of fatty acids affects the permeability of LFNs. While the permeability of LSNs was not significantly enhanced due to higher particle size after nanonization, LONs and LLNs increased 1.56 and 1.85 times in permeation, respectively, compared to LEU.

Conclusion: Utilization of different degree of saturation of fatty acids to conjugate a peptide drug could provide pharmaceutical versatility via self-assembly and modification of physicochemical properties.

Keywords: leuprolide acetate, hydroxyl targeted conjugation, different degree of saturation of C18 fatty acids, fatty acid-conjugated leuprolide, self-assembled nanoparticles, controlled release, enhanced permeability

Introduction

Peptide drugs have been used to treat chronic diseases. These drugs have several advantages including a high affinity for easy receptor binding, low immunogenicity, strong solubility, and low toxicity. In addition, they have excellent potential for pharmacological treatment through modification of synthesis characteristics.[1] The use of peptide drugs has gained much attention in research and development (R&D) in the pharmaceutical industry. It is estimated that 239 therapeutic peptides and proteins from 1980 to 2018 received FDA approval in the global market.[2] In addition, more than 150 clinical trials and 400–600 preclinical studies are in progress.[3]

Received: 2 January 2022
Accepted: 29 April 2022
Published: 17 May 2022

Leuprolide (LEU) is a synthetic 9-residue peptide analog of gonadotropin-releasing hormone (GnRH). LEU stimulates gonadotropin luteinizing hormone (LH) and follicle-stimulating hormone (FSH) present in the pituitary gland to increase ovarian and testicular steroid production, thus increasing estrogen levels in women and testosterone and dihydrotestosterone in men.[4] It is used as a treatment for sex hormone-dependent diseases such as endometriosis, uterine leiomyoma, precocious puberty, and prostate cancer. The goals of administering this drug to endometriosis patients are to reduce endometrial lesions and improve pelvic pain/tenderness and dysmenorrhea. In the case of uterine leiomyoma, LEU can reduce intraoperative bleeding by treating anemia before surgery, reducing the size of fibroids, and improving symptoms without surgery, and in precocious puberty, it slows the progression of secondary sexual characteristics.[5,6] LEU is administered by intramuscular injection; 3.75 mg for endometriosis and uterine leiomyoma patients and 7.5 mg once a month for prostate cancer.[7] However, these injections are associated with pain, burning, and tingling at the injection site, as well as whole body side effects such as headache, nausea, hot flushes, and night sweats.[8] Therefore, the finding of an alternative to the injectable of LEU has offered many challenges in recent years with pharmaceutical researchers. Herein, buccal or sublingual route of administration could be considered as an effective and non-invasive alternative to the injectable of LEU acetate for patient compliance, especially for children with precocious puberty.[9–11] On the other hand, the bioavailability of LEU is limited by poor permeability through biological membranes because of its low lipophilicity and limited intestinal absorption by proteases and peptidases.[3,12,13] In addition, LEU is rapidly degraded by chymotrypsin and has a short half-life.[14] Even though LEU has a relative good solubility in phosphate buffered solution (PBS) with approximately 10 mg/mL, due to its poor stability in pH 7.2–7.4 solution and blood, LEU can degrade or precipitate in the bloodstream, reducing blood circulation time. Table 1 shows physicochemical properties of LEU acetate.

To overcome these shortcomings, many studies are being conducted in the pharmaceutical industry. For example, technology for encapsulating LEU acetate in poly(lactic-co-glycolic-acid) (PLGA) microspheres[15,16] and PEGylation via conjugated LEU acetate and polyethylene glycol (PEG) has been developed.[17] Each of these technologies has its own advantages and disadvantages. First, PEGylation leads to improved drug solubility, drug stability, and increased residence time of the conjugate in blood; however, potential risks including immunogenicity of PEG-containing vacuoles have been

Table 1 Physicochemical Properties of LEU Acetate

Factors	Physicochemical Properties
2D structure	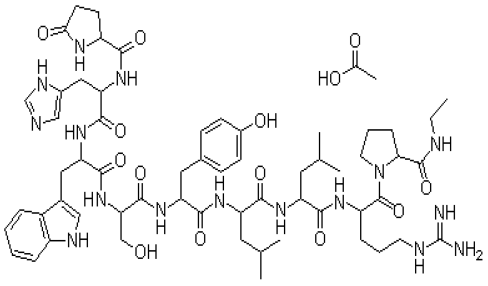
Molecular weight	1269.45 g/mol
Chemical formula	$C_{59}H_{84}N_{16}O_{12}.\ C_2H_4O_2$
BCS class	IV
Half life	1 mg intravenous administration: 3hr
Route of administration	IM injection
Dose strength	3.75, 7.5 mg per month
Solubility	≥ 66.66 mg/mL (52.51 mM) in water
log P	−2.7–1.07

observed.[18] Moreover, PLGA has excellent biodegradability, biocompatibility, and tunable mechanical properties, but it has low loading capacity for a more hydrophilic drug and a high initial burst release of small hydrophilic molecules.[19]

Recent fattigation platform technology has shown that amphipathic biomaterials, by conjugating biocompatible proteins such as gelatin, human serum albumin, transferrin, and fatty acids could provide therapeutic potentials for drug delivery.[20,21] More specifically, the conjugation of fatty acids and macromolecules could obtain the amphiphilic structures that could be self-assembled into nanoparticles. These amphiphilic structures can be used to effectively solubilize hydrophobic drugs by encapsulation of the drug in a hydrophobic inner core, from which the solubility and bioavailability of poorly water-soluble drugs will be significantly improved.[22] Therefore, in this study, we utilized the fattigation platform to conjugate LEU with fatty acids, forming an amphiphilic structure which could be easily self-assembled into nanoparticles. On the other hand, the utilization of long-chain fatty acids leads to better bioavailability through enhanced cellular uptake than short-chain fatty acids, and has sustained therapeutic effects through increased half-life and controlled release.[21,23] Long-chain unsaturated fatty acids are effective penetration enhancers for a variety of drugs. Among them, it was shown that the interaction of the stratum corneum (SC) and the penetration enhancer differs according to the different degree of saturation of fatty acids, in which the higher degree of unsaturation resulted in the higher permeability.[24]

The purpose of this study was to conjugate the hydroxyl groups of LEU acetate with different degree of saturation of C18 long-chain fatty acids (L18FCs), and to investigate the increased physicochemical properties of LEU for controlled release and improved permeability through the self-assembled nanonization process. There are two factors of fatty acids making them differ from one another, including carbon chain length and degree of saturation. In this study, we focused on investigating the conjugation of LEU with different degree of saturation of C18 fatty acids, aiming for noninvasive route of administration. Three types of L18FCs were selected: stearic acid (saturated, 0π), oleic acid (unsaturated, 1π), and linoleic acid (multi unsaturated, 2π). Table 2 gives physicochemical properties of different degree of saturation of C18 fatty acids selected for LEU conjugation. Each fatty acid conjugation (stearic acid-conjugated LEU acetate, LSC; oleic acid-conjugated LEU acetate, LOC; linoleic acid-conjugated LEU acetate, LLC) was synthesized by targeting fatty acids to the hydroxyl group of LEU acetate via the Yamaguchi esterification method and then purified using prep-HPLC. The physicochemical properties of the conjugated samples were analyzed by Fourier transform infrared (FT-IR) spectroscopy, differential scanning calorimetry (DSC), proton nuclear magnetic resonance (^{1}H-NMR), and matrix-assisted laser desorption/ionization-time of flight (MALDI-TOF). L18FNs (self-assembly nanoparticles of L18FCs) were characterized by dynamic light scattering (DLS), field emission scanning electron microscopy (SEM), and field-emission transmission electron microscopy (FE-TEM). Finally, a degradation test of L18FCs was performed in human plasma.

Table 2 Physicochemical Properties of Different Degree of Saturation of C18 Fatty Acids Selected for LEU Conjugation

Fatty Acids	Structure	Physicochemical Properties
Stearic acid	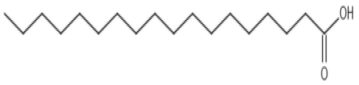	Chemical formula: $C_{18}H_{36}O_2$ Features: C18, saturated Molecular weight: 284.48 g/mol Melting Point: 69.3°C log P: 8.23
Oleic acid	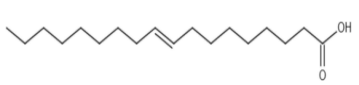	Chemical formula: $C_{18}H_{34}O_2$ Features: C18, mono-unsaturated Molecular weight: 282.47 g/mol Melting Point: 13.4°C log P: 7.64
Linoleic acid	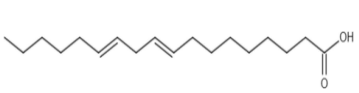	Chemical formula: $C_{18}H_{32}O_2$ Features: C18, polyunsaturated Molecular weight: 280.45 g/mol Melting Point: −5°C log P: 7.05

Materials and Methods

Materials

LEU acetate was used as a drug purchased from Anygen (Kwangju, Korea). Stearic acid, oleic acid, linoleic acid were used as fatty acids purchased from Sigma-Aldrich (Saint Louis, MO, USA). Benzoyl chloride was used as a chemical intermediate, triethylamine as a catalyst and acid neutralizer, and 4-Dimethylaminopyridine (DMAP) as a coupling reaction agent (Sigma-Aldrich). Phosphate-buffered saline tablets and sodium hexanesulfonate used in the degradation studies were purchased from Sigma-Aldrich. A dialysis membrane (MWCO: 1000 Da) was purchased from Spectrum Labs (San Francisco, CA, USA) and used for purification. 2,5-Dihydroxybenzoic acid (DHB) and α-cyano-4-hydroxycinnamic acid were used as matrices for MALDI-TOF (Sigma-Aldrich). Peptide calibration standard II was used for matrix-assisted laser desorption and ionization (Bruker, Billerica, MA, USA). A PB-M membrane was used as a permeation barrier membrane (UMC Science, Goyang, Korea). Isopropyl myristate was used as a membrane activator (Sigma-Aldrich Saint Louis, USA). Tetrahydrofuran (THF), 99.5% absolute ethanol, HPLC-grade methanol, and trifluoroacetic acid (TFA) were purchased from Samchundang (Seoul, Korea).

Preparation of Hydroxyl Group-Targeted L18FCs

Synthesis of L18FCs

LEU acetate (127 mg) was dissolved in 4 mL of deionized water (DW) and stirred at 700 rpm until completely dissolved. Then, 14 µL of triethylamine was dissolved in LEU acetate solution to desorb the acetate anions. C18 fatty acids (25 mM) were dissolved in 4 mL of THF and stirred at 700 rpm until completely dissolved. To deprotonate the carboxylic group of fatty acids for the reaction, triethylamine (14 µL) was added into fatty acids/THF solution and followed by the adding of benzoyl chloride (12 µL) and DMAP (1.22 mg). Herein, the deprotonated fatty acids reacted with benzoyl chloride to form the acid anhydride. Then, the obtained acid anhydride was attacked with DMAP, forming another leaving group (fatty acid-DMAP reactive) and then it was replaced by the hydroxyl group of LEU. Yamaguchi chloride (2,4,6-tribenzoyl chloride) used in the existing mechanism causes steric hindrance, therefore benzoyl chloride was used instead.[25] Figure 1 shows a schematic diagram for the hydroxyl group targeted LEU-oleic acid conjugate (LOC). After

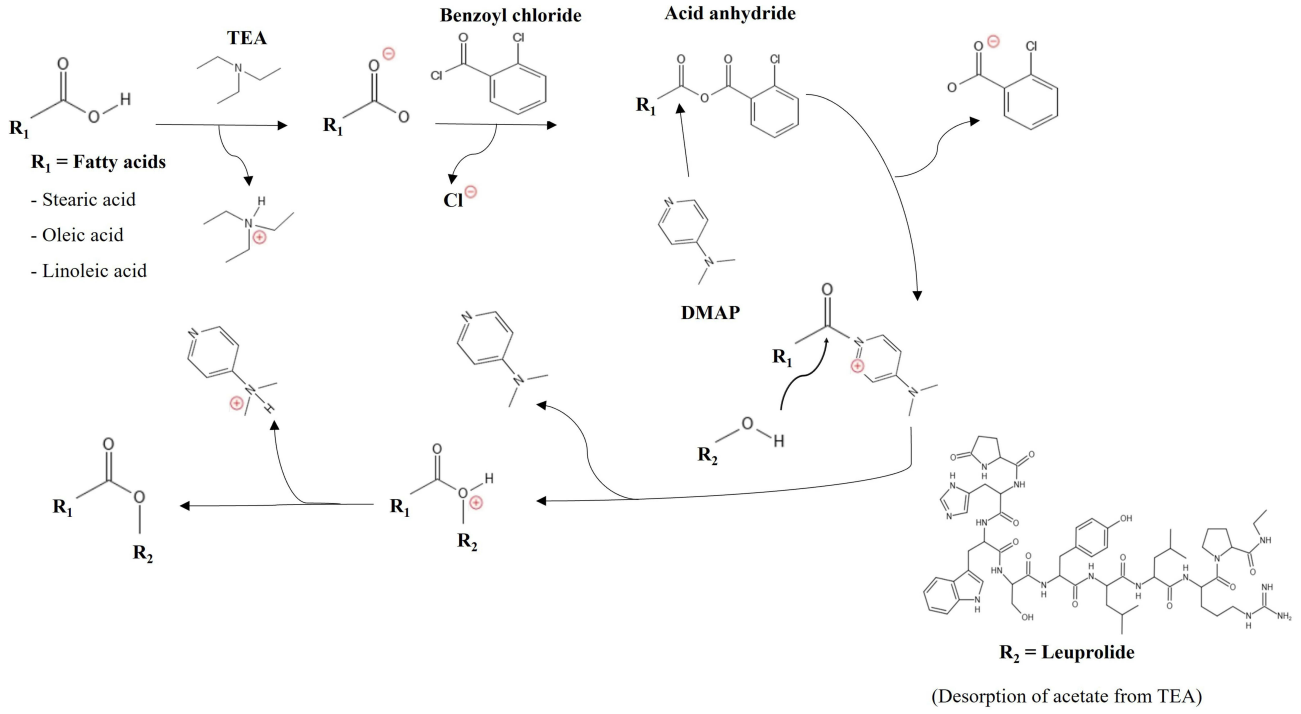

Figure 1 Schematic diagram for the hydroxyl group targeted LEU-oleic acid conjugate (LOC).

stirring for 1 h, the mixture was injected into the DW through a 0.45 μm PTFE syringe filter (Whatman, England) and stirred at 700 rpm for 3 h. Finally, the solution was dialyzed against absolute ethanol to purify the unreacted substances.

Purification by Prep-HPLC

The conjugation sample was dissolved in 20 mL of acetonitrile (ACN). Then, the sample was sonicated for 5 min and filtered through a 0.45 μm PTFE syringe filter (Whatman, England). The preparative HPLC separation was performed by injecting 20 mL of the filtered extract onto a YMC-Pack C18 column AA30S05 (20 × 250 mm, 30 nm, 5 μm) semi-preparative ODS-A HPLC column (YMC, Japan). Elution was performed using a Waters model DeltaprepLC300 and pumps to deliver a constant flow rate of 10 mL/min, and the column temperature was maintained at room temperature (^{o}C). The mobile phase consisted of A and B; mobile phase A: DW with 0.1% TFA and B: ACN with 0.1% TFA. The solvent system consisted of 50% ACN in DW for 15 min and then changed linearly over 35 min to 70% ACN. The percentage of ACN was then increased to 100% over 10 min and isocratically run for 5 min. Table 3 shows composition gradients of Prep-HPLC system. The L18FCs were detected by absorbance at 220 nm using a Waters 2487 tunable absorbance detector. LSC was collected between 23 and 30 min, LOC was collected between 21 and 27 min, and LLC was collected between 19 and 23 min. The collected samples were evaporated in organic solvents by rotary evaporation (N-1100, Eyela, Japan), and made into a powder form by freeze-drying (FD8518, Ilshin Biobase, Korea).

Identification and Physicochemical Characterization

Nuclear Magnetic Resonance (NMR) Spectroscopy

LEU acetate, C18 fatty acids, and L18FCs were dissolved in DMSO-d6 at a concentration of 10 mg/mL. ^{1}H-NMR spectra were analyzed using an AVANCE II 400 (Bruker, USA) 400 MHz spectrometer at 25°C.

Matrix-Assisted Laser Desorption/Ionization-Time of Flight (MALDI-TOF)

A mixture of 375 μL of 50% ACN and 375 μL DW and 0.1% TFA in a 1:1 ratio was created in an EP tube (total volume = 1 mL). After injecting 500 μL of the prepared mixed solution into another EP tube, 10 mg of α-cyano-4-hydroxycinnamic acid (CHCA) was added and dissolved. The remaining mixture (250 μL) was injected into an EP tube containing 5 mg DHB and vortexed for 1 min. Two microliters of peptide calibration standard II solution and 2 μL of CHCA solution were mixed in an EP tube to make a standard on the plate. Then, 2 μL of the sample obtained via preparative HPLC (ACN 59.5 to 66.25%) and 2 μL of DHB solution were removed and placed into an EP tube and one drop was then placed on the plate. Finally, the plate was placed in the device and analyzed. MALDI-TOF experiments were performed using an Autoflex maX® (Bruker, Billerica, USA).

Fourier Transform-Infrared (FT-IR) Spectrometer

LEU acetate, C18 fatty acids, the physical mixtures, and conjugation samples were analyzed using an FT-IR spectrometer (Nicolet iS550, Thermo Fisher, Japan) to determine the conjugation synthesis between LEU acetate and C18 fatty acids, as well as the properties of each substance. The spectrum range was 400–4000 cm^{-1}, and the resolution was recorded as 4 cm^{-1}.

Table 3 Composition Gradients of Prep-HPLC

Time (min)	DW (%)	ACN (%)
0	80	20
15	50	50
35	30	70
45	0	100
50	0	100

Differential Scanning Calorimetry (DSC)

The peaks and quantity of heat change were confirmed to establish the physicochemical properties of LEU acetate, C18 fatty acids, the LEU acetate and C18 fatty acid physical mixture, and L18FCs using a DSC 200 F3 Maia (Netzsch, Germany). Each sample was analyzed by weighing 5 mg, sealed within the aluminum pans, and heated from −20°C to 180°C at a heating rate of 10°C/min, with nitrogen gas used for the purge process. Heat flow and temperature calibrations were performed using indium.

Formation and Characterization of Self-Assembled Nanoparticles

Dynamic Light Scattering (DLS)

L18FNs were analyzed for size, distribution, and surface zeta potential using DLS (ELSZ-2000 S, Otsuka Electronics, Japan). For converting L18FCs into L18FNs, 10 mg of conjugates is dissolved in 2 mL absolute ethanol, and then 10 mL of DW was slowly added and stirred at 700 rpm at room temperature (25 °C) overnight. After solvent evaporation, L18FNs were obtained and each sample was analyzed in triplicate.

Field Emission Scanning Electron Microscope (FE-SEM)

The size and morphology of LEU acetate and L18FNs were observed using FE-SEM (JSM-7900F, JEOL, Japan). A drop of the sample was placed on a copper grid-covered carbon tape. The solution samples were dried in a vacuum at room temperature (25 °C) for 24 h and then coated with platinum for 1 min in a vacuum.

Field Emission Transmission Electron Microscope (FE-TEM)

The size and morphology of the L18FNs were observed by FE-TEM (Tecnai G2 F30 S-Twin, Philips-FEI Corp., Best, Netherlands). Samples were stained with 2% PTA solution. Then, a drop of each sample was placed on a TEM copper grid and dried in an oven at 37°C for 24 h.

Controlled Release and Degradation Profile of LEU-Fatty Acid Conjugates

Purified L18FCs (10 mg) and LEU (10 mg) were dissolved in 500 μL DMSO. Then, 100 μL of each of these solutions was injected into 1.9 mL of human plasma at 37°C at 100 rpm in a water bath (BS-06, JEIO TECH, Korea). After mixing with human plasma, the concentration of L18FCs or LEU was 1 mg/mL. At specified time points, 100 μL of the mixture was withdrawn and mixed with 900 μL of cold MeOH (approximately 0.1 mg/mL of L18FCs or LEU after dilution), and the mixture was vortexed for 1 min to stop the hydrolysis reaction. For the first time point (0 min), 900 μL of cold MeOH was added immediately into the withdrawal after mixing with human plasma. Next, the samples were centrifuged for 10 min at 10,000 rpm, and the supernatants were analyzed by HPLC (n=3).

The HPLC system (Agilent 1200, Agilent Technologies, USA) consisted of a pump, a diode-array detection (DAD), and a reverse-phase column (Poroshell 110 Å, C18 column, 250×4.6 mm, 5 μm, Phenomenex Gemini®). The analysis was performed isocratically, and the mobile phase was divided into two types, A and B. For LEU acetate, mobile phase A was 10 mM sodium hexanesulfonate composed of acetonitrile: DW = 32:68 (v/v) with 0.1% TFA. For L18FCs, mobile phase B was 10 mM sodium hexanesulfonate in acetonitrile: DW = 68:32 (v/v) with 0.1% TFA. The analysis experiment was performed at a flow rate of 1.0 mL/min, an injection volume of 30 μL, and the temperature of the column was set to room temperature (25 °C). The LEU acetate peak was detected at 8.98 min through mobile phase A. The LSC peak was detected at 11.70 min, the LOC peak at 6.98 min, and the LLC peak at 5.37 min through mobile phase B.

In vitro Permeability of LEU-Fatty Acid Nanoparticles (L18FN)

In vitro permeation studies were performed in a standard diffusion cell with a diffusion area of 3.8 cm^2 (DHC-6TD, Logan, USA). The permeation barrier membrane (PB-M) was clamped between the donor and the receiving compartments. PB-M was soaked in isopropyl myristate solution overnight as a pretreatment for membrane activation. LEU was prepared by dissolving 5 mg and 10 mg of LEU in 10 mL of pH 6.8 buffer solution. L18FCs were nanonized in pH 6.8 buffer solution under the same conditions as previously described. The donor cell was filled with 300 μL of each sample

(LEU or L18FNs) and the receiving compartment was filled with 5 mL of PBS (pH 7.4) containing 0.5% Tween 80 and stirred continuously at 600 rpm using a magnetic stirrer. The entire device was maintained at 37°C using a jacket surrounding the cells. Samples (500 µL) were withdrawn at 15, 30, 60, 120, 240, 360, 480, 600, and 720 min and recharged with 500 µL of receiving compartment solution at 37°C. HPLC analysis was performed under the same conditions as those in the previous degradation test (n=3).

Results and Discussion

Fattigation Background of LEU-Fatty Acid Conjugates

In this study, the pharmaceutical limitations of LEU in drug delivery were overcome by utilizing a fattigation platform in which the hydroxyl groups of LEU acetate were conjugated with different degree of saturation of C18 fatty acids for the following advantages. (1) Human serum albumin (HSA) is one of the major protein components of plasma, with seven common fatty acid-binding sites. When bound to HSA, the molecule is sterically protected from proteolysis and rapid renal filtration because of the relatively large HSA size of approximately 66 kDa. After binding to HSA, the molecule is gradually released into the circulation, which can help increase blood circulation.[26] (2) The conjugate of hydroxyl groups of LEU and fatty acids was able to form self-assembled LEU nanoparticles according to specific synthetic conditions (pH, temperature, and solvent). It can inhibit the degradation rate of protease in the bloodstream and increase the half-life of LEU by maintaining its function.[27] (3) Self-assembled nanonization of amphiphilic peptide conjugates with different degree of saturation of fatty acids has potential advantages for modulating and improving the permeability of LEU analogues as compared to LEU acetate as compared to LEU.[28]

Synthesis and Identification of LEU-Fatty Acid Conjugates

The prepared samples were purified using only hydroxyl-group one-targeting substances through Prep-HPLC. The synthesis of these substances was confirmed, and the changes in physicochemical properties were analyzed. ^{1}H-NMR spectra of LEU, fatty acids and LEU-fatty acid conjugate via esterification having different saturation levels is shown in Figure 2. In the NMR spectrum of each fatty acid, a CH_2 stretch peak at around 1.2 ppm and a carboxyl group peak at approximately 12 ppm were observed in the NMR spectrum of each fatty acid. In the case of unsaturated fatty acids such as oleic and linoleic acid, double bonds were observed at 5.3 ppm.[29] It can be seen that the CH_2 peak and the double bond peak of the unsaturated fatty acid occurred, and the peak of the carboxyl group disappeared. Evidence for esterification of the synthesis of LEU and fatty acids was the signal of the methoxy group of the methyl ester (CH_2-OCO) at 3.65 ppm. A significant difference in the peaks of LEU and L18FCs (LSC, LOC, LLC) was observed.

Additionally, the conjugation of different degree of saturation of fatty acids with LEU acetate was analyzed by MALDI-TOF. Figure 3 MALDI-TOF results of LEU-fatty acid conjugate after purification by Prep-HPLC. LEU acetate loses its acetate structure due to desorption by TEA. When conjugation with each fatty acid occurs, water molecules are removed from the esterification reaction. Calculating the theoretical molecular weight of this point, the molecular weights were as follows: LSC is 1475.8 g/mol, LOC is 1473.8 g/mol, and LLC is 1471.78 g/mol. As shown in Figure 4, the molecular weight is consistent with the calculation results. Since these resultant products were purified through Prep-HPLC, there were no residual LEU and byproducts.

Figure 4 shows FT-IR spectra of LEU acetate, fatty acids, physical mixtures, and LEU-fatty acid conjugate having different saturation levels (LSC, LOC, and LLC). As a result of LEU acetate, the O-H bond peak appeared at 3274 cm^{-1}, and the C=O stretch peak appeared at 1624 $cm.^{-1}$ [30] In the order of stearic acid, oleic acid, and linoleic acid, CH_2 stretching appeared at 2845 and 2914 cm^{-1} (stearic acid), 2853 and 2922 cm^{-1} (oleic acid), 2853, 2923 and 3008 cm^{-1} (linoleic acid), and in the case of carboxyl group, 1695 cm^{-1}, 1707.93 cm^{-1}, and 1707.75 cm^{-1}, respectively. The shifting of the -OH group into 3285 cm^{-1} for LSC, 3282 cm^{-1} for LOC, and 3286 cm^{-1} for LLC evidenced for esterification of these conjugates. The esterification reaction also occurred at the C=O stretch site of LEU acetate, positioning at 1651 cm^{-1} for LSC and LOC, and 1645 cm^{-1} for LLC. Lastly, CH_2 stretches of existing fatty acids also showed a peak shift of 2853, 2924 cm^{-1} for LSC, 2855, 2927 cm^{-1} for LOC, and 2860, 2930,

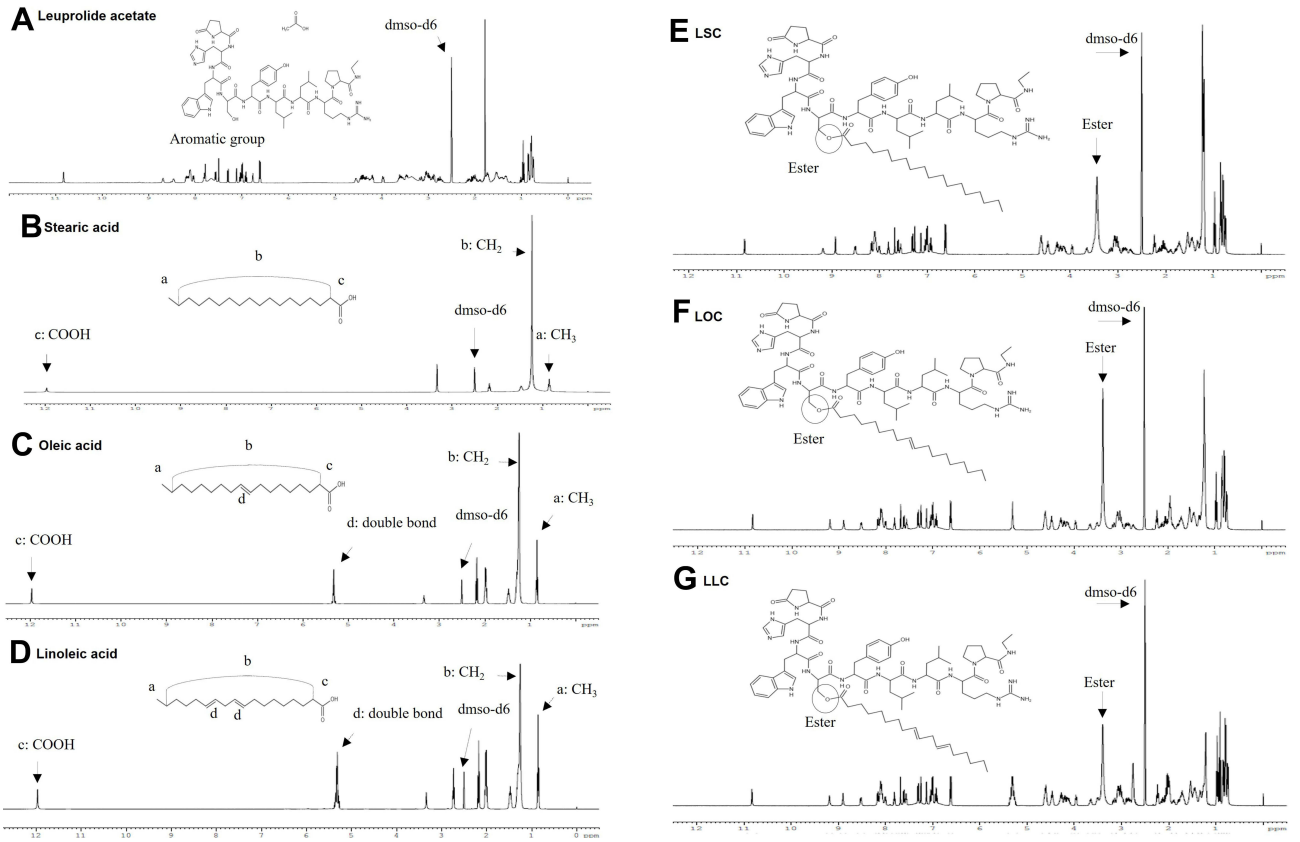

Figure 2 ^{1}H-NMR spectra of LEU, fatty acids and LEU-fatty acid conjugate having different saturation levels: (**A**) LEU acetate, (**B**) Stearic acid, (**C**) Oleic acid, (**D**) Linoleic acid, (**E**) LSC, (**F**) LOC, (**G**) LLC.

3015 cm^{-1} for LLC. Collectively, it was found that the physicochemical properties were changed through the conjugation of LEU acetate and fatty acids.

Physicochemical Characterization of LEU-Fatty Acid Conjugates

Figure 5 shows DSC thermograms of LEU acetate, fatty acids, physical mixtures, and LEU-fatty acid conjugate having different saturation levels. The endothermic peaks of LEU acetate were characterized at 76.4°C and 162.5°C, and at 73.1°C for stearic acid, 17°C for oleic acid, and −6.1°C for linoleic acid. There was no significant difference in the endothermic peak between each fatty acid and the physical mixture. All the conjugation samples had a similar pattern to that of LEU acetate, but it could be seen that an endothermic peak shift occurred. In the case of LSC, the peaks shift was at 66.7°C and 147.2°C, in the case of LOC at 81°C and 126°C, in the case of LLC at 76.6°C and 120.4°C. It was confirmed that higher degree of unsaturation of fatty acids narrowed the interval between the endothermic peaks of the L18FCs as compared to LEU.

Physicochemical Characterization of Self-Assembled Nanoparticles

The particle size, polydispersity index (PDI), and zeta potential values of self-assembled L18FNs analyzed by DLS are presented in Table 4. The resulting nanoparticles sizes are as follows: LSNs: 180.11 ± 11.27 nm, LONs: 144.47 ± 7.49 nm, and LLNs: 79.9 ± 0.40 nm. As the degree of unsaturation increases, it can be seen that the size of the nanoparticles decreases. The diameter of the peptide drugs had a significant effect on the absorption of nanoparticles. M cells, specialized epithelial cells of mucosal-associated lymphoid tissue, preferentially transport particles at small (20–100 nm) but also at larger sizes (100–500 nm).[31] The resulting zeta potentials are as follows: LSNs: 31.24 ± 4.12 mV, LONs: 57.13 ± 2.17 mV, and LLNs: 76.13 ± 1.32 mV. The high absolute values of the zeta potential indicated the good stability of nanoparticles.[31] Herein, we continued measuring the critical aggregation concentration (CAC) of three L18FCs in deionized water to

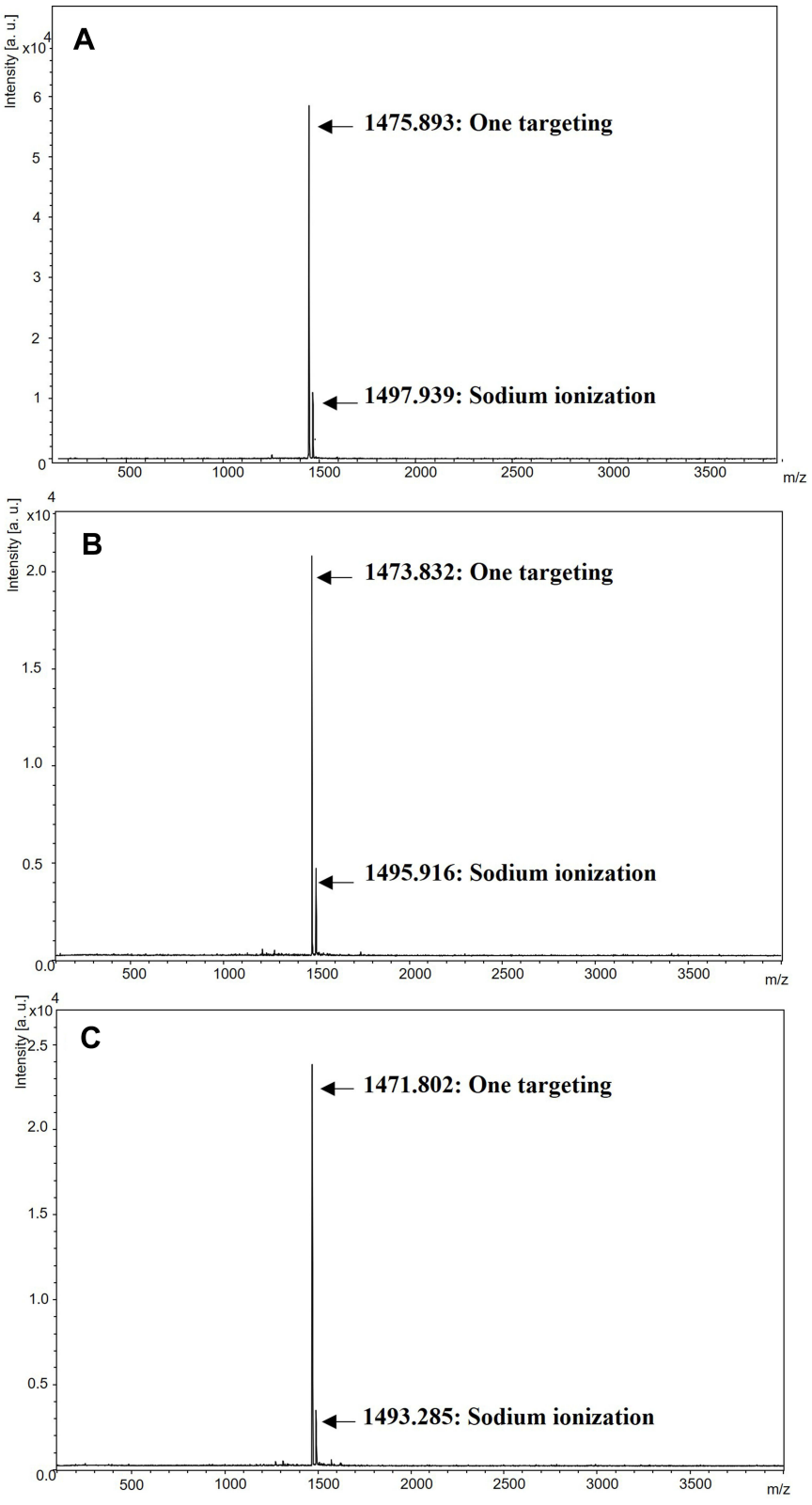

Figure 3 MALDI-TOF results of LEU-fatty acid conjugate after purification by Prep-HPLC: (**A**) LSC, (**B**) LOC, (**C**) LLC.

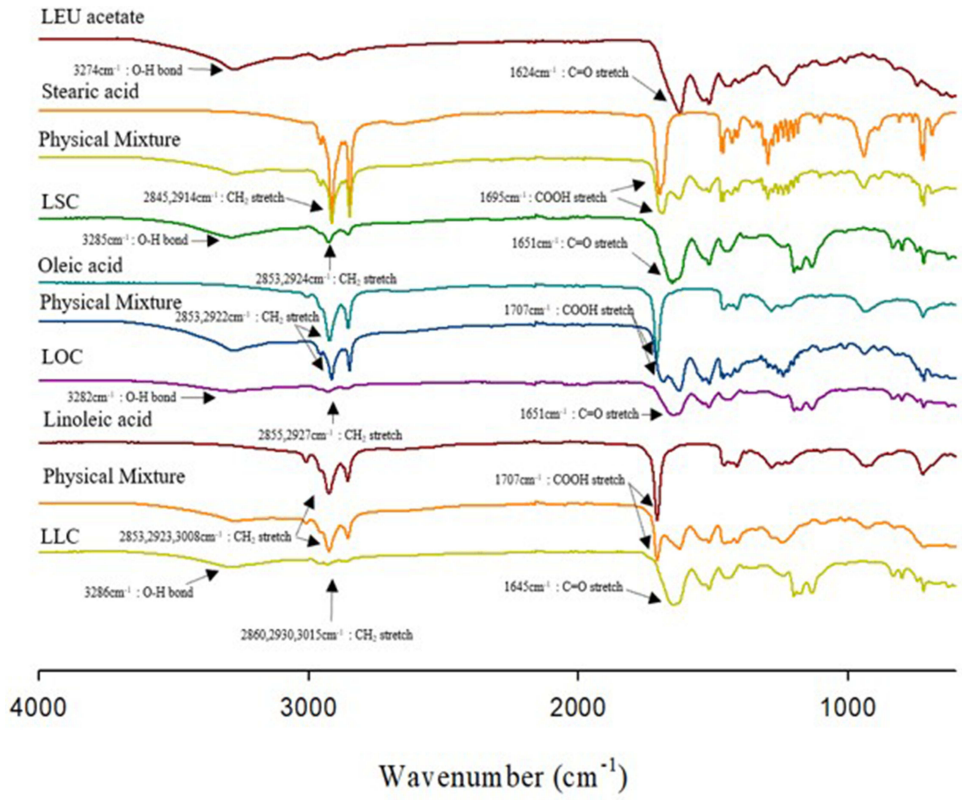

Figure 4 FT-IR spectra of LEU acetate, fatty acids, physical mixtures, and LEU-fatty acid conjugate having different saturation levels (LSC, LOC, LLC).

evaluate the effect of different degree of saturation of fatty acids on the aggregability of each conjugate. Figure S1 and the Supplementary materials "Critical Aggregation Concentration (CAC) Measurement" section show CAC values of LSC, LOC and LLC. As a result, there was a trend in the CAC values related to the degree of saturation of conjugated fatty acids. LSCs showed the lowest CAC at 6.76 μg/mL as compared to LOC and LLC (12.18 and 14.12 μg/mL, respectively), which indicated that LSC had the strongest aggregability due to the absence of the double bond in the fatty chain. Thereby, there was a connection between the saturation level of a fatty acid and the CAC of the obtained conjugate. In addition, it was found that the higher the degree of unsaturation, the higher the zeta potential value. Herein, it was noted that there was a relationship between the CAC and self-assembly of the nanoparticles. At the same concentration above CAC, the conjugate with a higher CAC value would obtain the nanoparticles with larger particle size and smaller potential value due to the stronger aggregability. Interestingly, it is reported that cationic compounds have a positive effect on dermatology from a percutaneous penetration point of view. This is because the skin is negatively charged due to phosphatidylcholine and carbohydrates and contains negatively charged groups at neutral pH. Then, it can aid the transportation of nanoparticles from the blood–brain barrier. Therefore, the obtained L18FNs with high absolute values and positive charges could provide a key role for the enhanced permeability.

Figure 6 visualizes FE-SEM images of LEU acetate and self-assembled L18FNs. Figure 7 also shows FE-TEM images of self-assembled L18FNs having different saturation levels. Evidently, the spherical nanoparticles could be confirmed through self-assembly. Comparing the SEM image results of LSNs and LLNs, this can be seen a significant difference in aggregation of nanoparticles due to the difference in saturation level of fatty acids. Conjugated with the saturated fatty acid, stearic acid, showed high aggregation of nanoparticles due to its higher hydrophobicity and lower CAC value, while unsaturated fatty acids showed less aggregation with smaller size of the obtained nanoparticles. Collectively, it can be seen that the particle size and morphology of L18FNs are different according to the saturation level of each conjugated fatty acid.

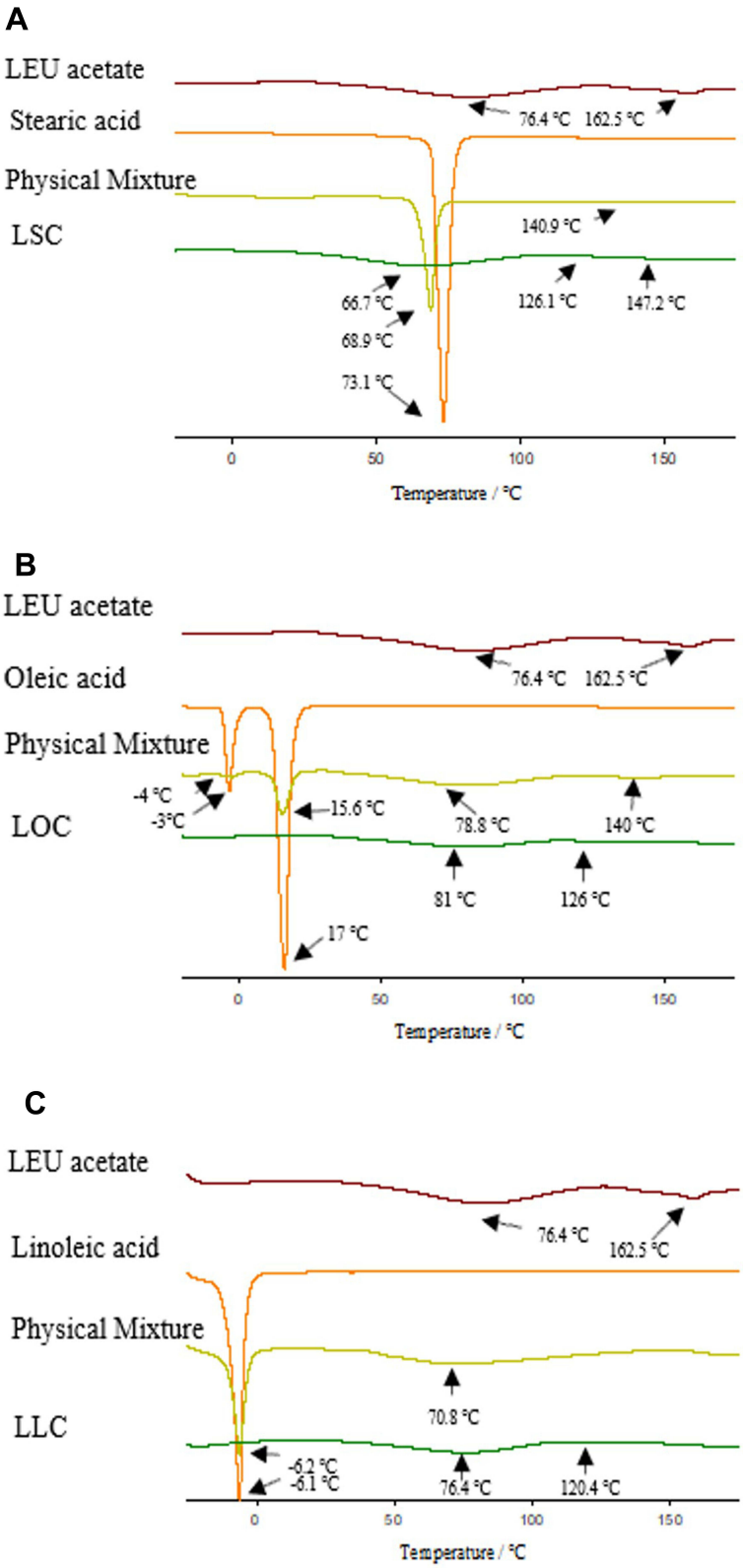

Figure 5 DSC thermograms of LEU acetate, fatty acids, physical mixtures, and LEU-fatty acid conjugate having different saturation levels: (**A**) LSC, (**B**) LOC, (**C**) LLC.

Table 4 Physicochemical Properties of Self-Assembled L18FNs

Nanoparticle	Particle Size (nm)	Polydispersity Index	Zeta Potential (mV)
LSN	180.11 ± 11.27	0.446 ± 0.108	31.24 ± 4.12
LON	144.47 ± 7.49	0.285 ± 0.028	57.13 ± 2.17
LLN	79.9 ± 0.40	0.144 ± 0.017	76.13 ± 1.32

Note: Mean ± standard deviation (n=3).

Controlled Release and Degradation Profile of LEU-Fatty Acid Conjugates

Degradation profiles of LEU and L18FCs, and conversion profiles from L18FCs to cumulative LEU concentration in human plasma are given in Figure 8 for long-acting drug delivery property and controlled release of LEU. LEU itself exhibits slow degradation and low drug potency, with approximately 45.75% of the drug degraded in the human plasma used in the experiment within 35 days. It can be seen that the degradation rates differed according to saturation levels of conjugated fatty acids. From this hydrophobicity, 99.33% degradation was found at 5 weeks for LSC, 99.56% degradation at 4 weeks for LOC, and 99.48% degradation at 4 weeks for LLC. Even though LOC and LLC showed the degradation process extended in the same period (5 weeks), 50% of LOC was degraded within 1.5 d, whereas LLC was degraded by 50% in just 0.89 days, with a difference of approximately 0.61 days between LOC and LCC. In addition to this comparison, it was 3.15 days for LSC, which was approximately 3.54 times longer than that of LLC, showing a slow degradation of LSC. If the rate of degradation was too fast, the rapid release may occur and a sustained release profile will be prohibited. Conversely, if the degradation rate is too slow, it was difficult to achieve an adequate drug efficacy.[32] Therefore, the release of LEU converted from L18FCs was controlled by the conjugation of different saturation level of fatty acids. In addition, as depicted in Figure 8, the concentration of LEU

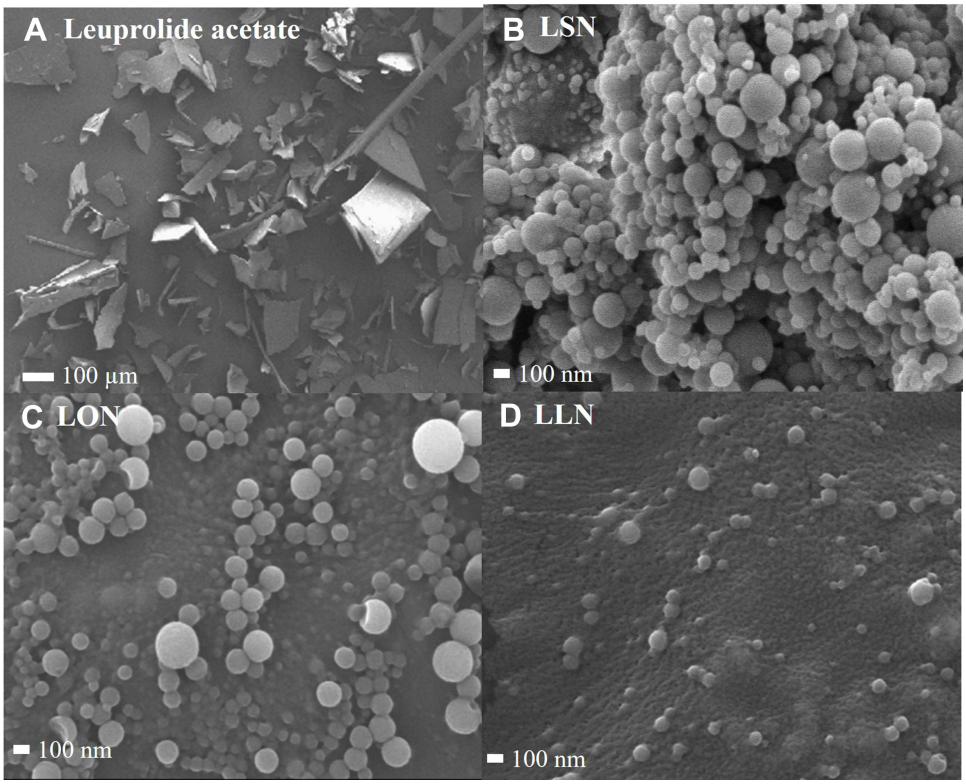

Figure 6 FE-SEM images of LEU acetate and self-assembled L18FNs: (**A**) LEU acetate, (**B**) LSN, (**C**) LON, (**D**) LLN.

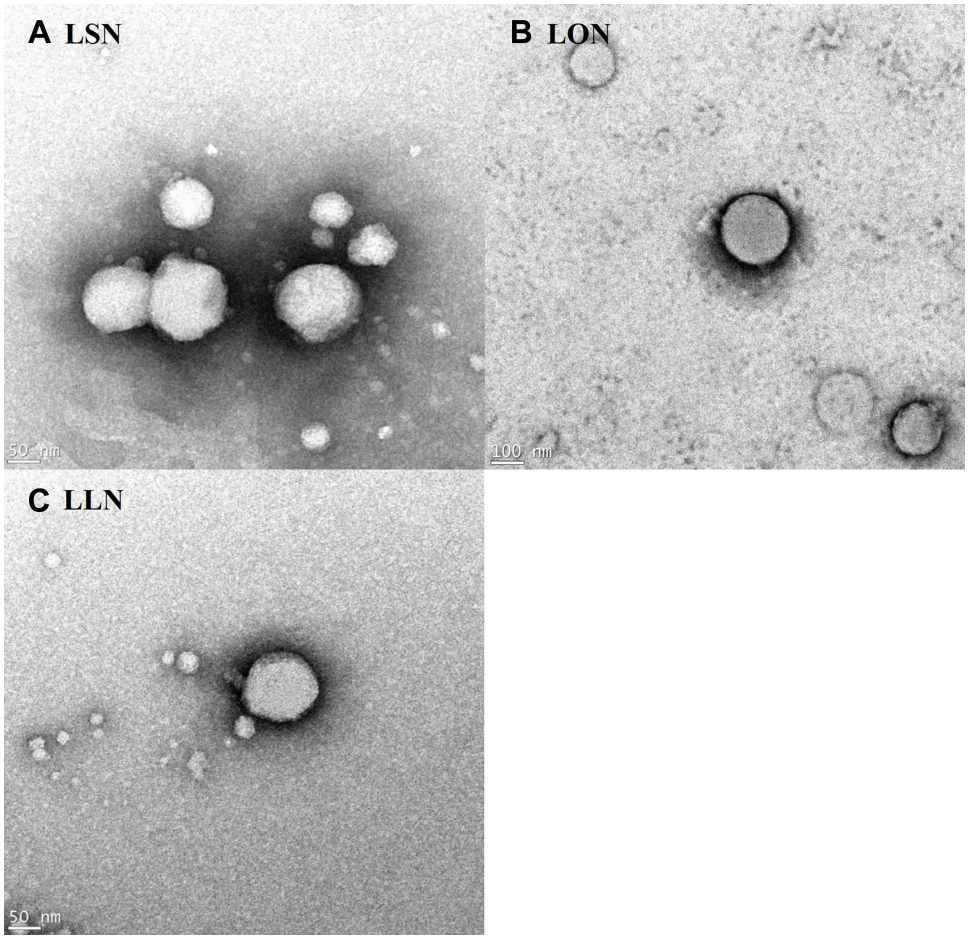

Figure 7 FE-TEM images of self-assembled L18FNs: (**A**) LSN, (**B**) LON, (**C**) LLN.

obtained from the decomposition of each L18FC accumulated at 80.26% at 5 weeks for LSC, while the LEU concentration converted from LOC and LLC had accumulated at 83.43% and 85.5% at 4 weeks, respectively. As a result, it was confirmed that the higher degree of unsaturation of a fatty acid promoted a faster degradation of its conjugate following by the higher amount of accumulated drug release. Referring to the degradation rate (%) of LEU, it could be seen that L18FCs were continuously released as they were converted to LEU, thereby reducing drug loss.

In vitro Permeability of LEU-Fatty Acid Nanoparticles

Figure 9 shows permeability profile of LEU (0.5 mg/mL and 1 mg/mL) and L18FNs as a function of time in pH 7.4 PBS through permeation barrier-membrane (PB-M) using a Franz diffusion cell method. LEU showed a permeability of 17.8% for 12 h at 0.5 mg/mL LEU concentration, and in the case of 1 mg/mL the permeability was 24.26%. These results confirmed that the higher the drug concentration, the higher the permeability of the cellulose membrane. The permeability of nanoparticles after nanonization from LEU-fatty acid conjugates varied according to the different saturation levels of fatty acids. All samples showed the highest permeability between 120 and 240 min. In the profiles of L18FNs, the permeability of LSN was 17.51%, which was about 6.75% lower than that of the existing drug LEU. This could be because the long-chain saturated fatty acids make the membrane more rigid and the permeability decreases due to reduced fluidity.[33] In contrast, the conjugation of LEU with unsaturated fatty acids showed the improvement of permeability, with 37.85% and 44.85% of LON and LLN permeation, respectively. Compared with the permeability of LEU, the permeability increased by 1.56

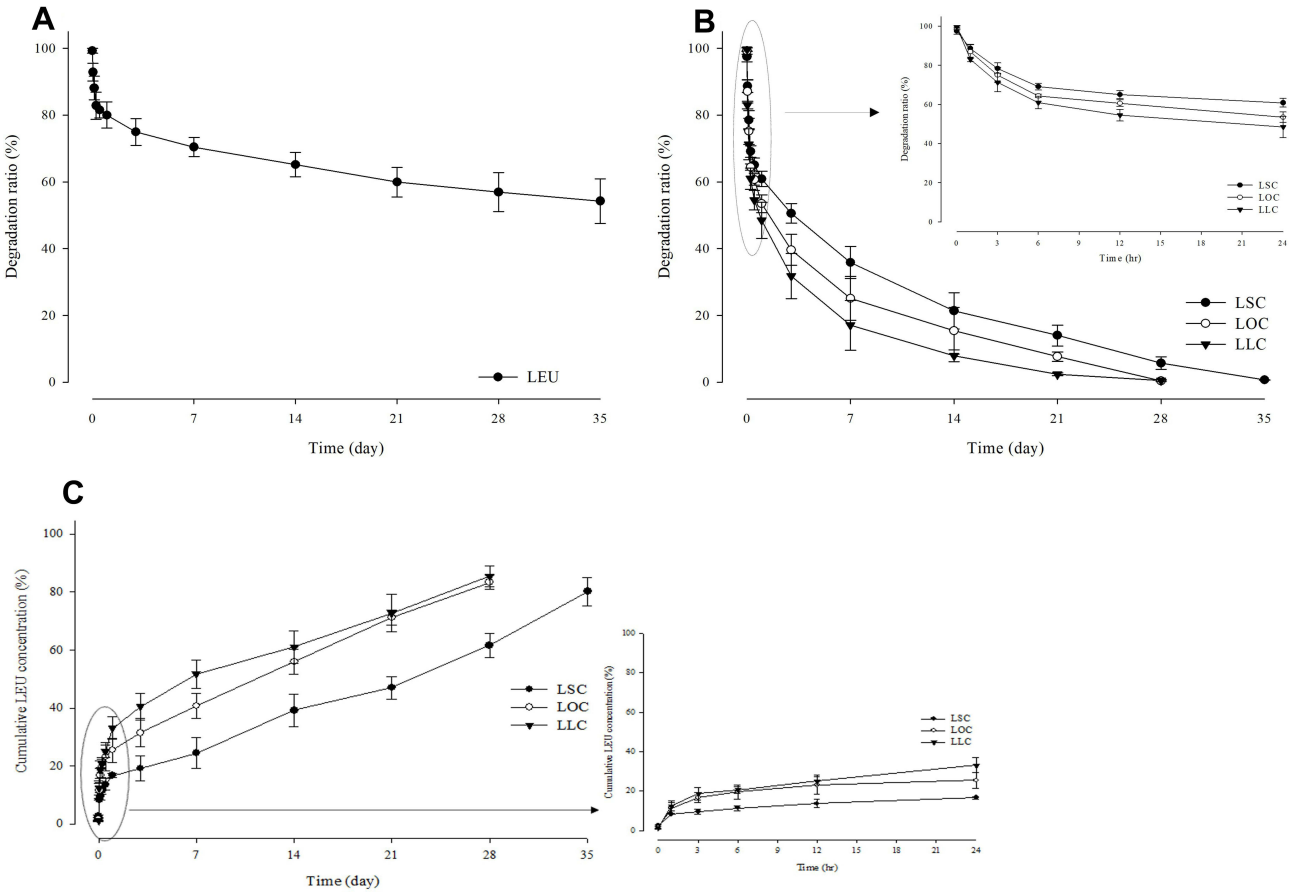

Figure 8 Degradation profiles of LEU (**A**) and L18FCs (**B**), and conversion profiles from L18FCs to cumulative LEU concentration (**C**) in human plasma (n=3).

times for LON and 1.85 times for LLN. This increase in permeability is considered because the cis double bonds present in unsaturated fatty acids can cause kinking of alkyl chains, which can interfere with stratum corneum lipid packing.[34] In addition, it has been confirmed that the smaller the nanoparticle size, the higher the skin permeation efficiency, which can affect the observed results.[35] To confirm the penetration phenomena of self-assembled nanoparticles, Figure 10 visualizes FE-SEM images of the PB-M surface before and after 120 min from the treatment of LON in permeation test. It was noted that the highest permeability of LON occurred between 120 and 240 min. From the images of LON penetrating PB-M, the small-sized self-assembled nanoparticles were preferentially permeated.

Conclusions

The LEU conjugation via esterification reaction was successfully targeted to the hydroxyl group of LEU. The changes in physicochemical properties due to esterification were analyzed by FT-IR, ^{1}H-NMR, DSC, and MALDI-TOF. The self-assembled nanoparticles formed when L18FCs were dispersed in a solvent, showing a smaller particle size and higher zeta potential in the unsaturated state than those in the saturated state. These self-assembled nanoparticles according to the C18 fatty acid saturation levels significantly affected the physicochemical properties, mainly degradation rate and permeation. It was confirmed that the higher amount of double bonds is presented in the fatty acids, the higher permeability of conjugates is achieved. Conjugation with different degree of saturation of fatty acids in the degradation tests also showed different degradation kinetics in a controlled manner for long-acting LEU efficacy. The hydroxyl group targeted LEU conjugation and self-assembled nanonization process can be applicable for enhanced drug delivery, aiming

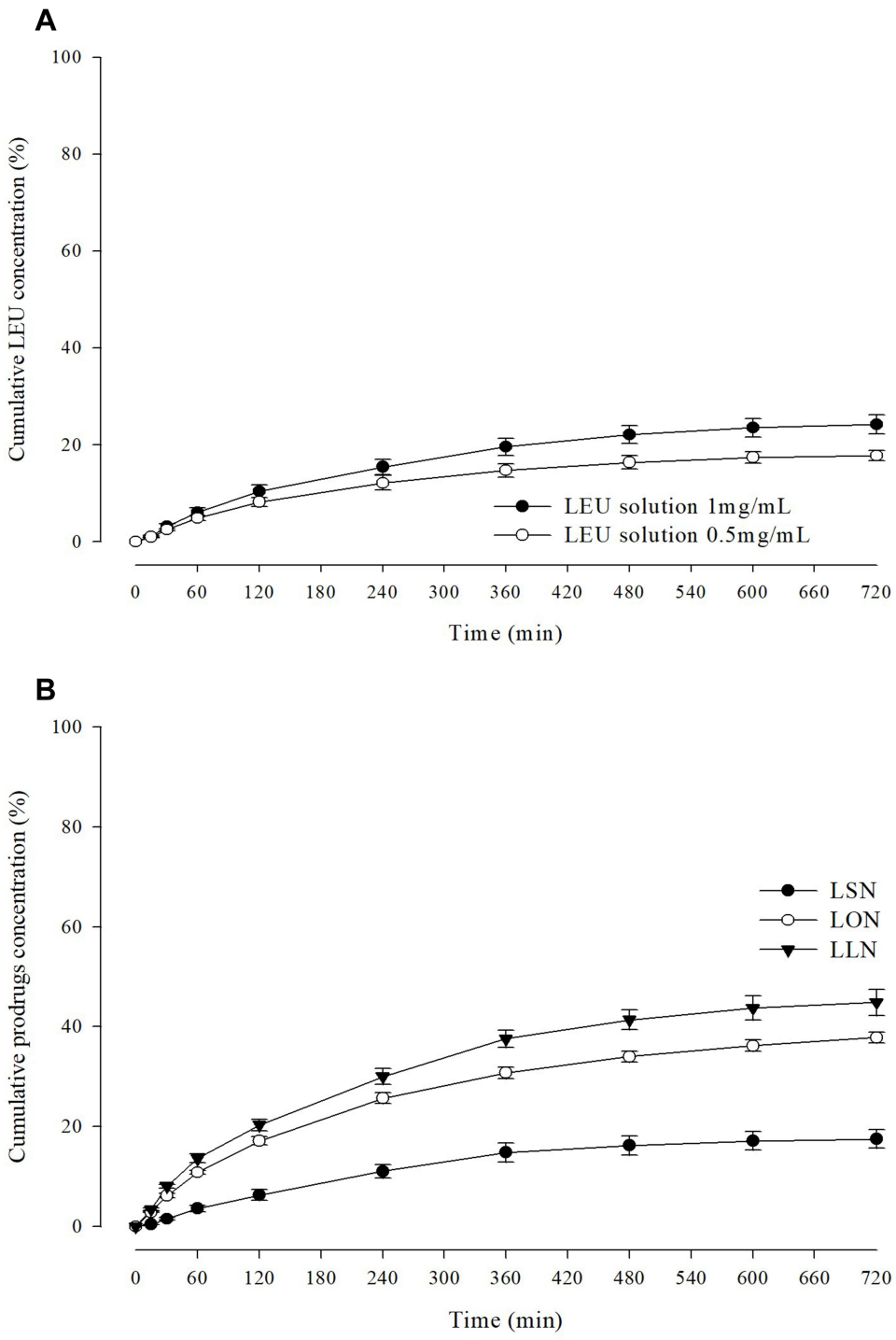

Figure 9 Permeability profile of LEU (**A**) and L18FNs (**B**) as a function of time in pH 7.4 PBS through permeation barrier-membrane (PB-M) using Franz diffusion cell (n=3).

for noninvasive buccal delivery to substitute invasive parenteral LEU injectable. The availability of the fattigation platform technology could be also challenged for peptide and protein medicine like LEU to improve drug delivery properties by increasing the lipophilicity and self-assembly.

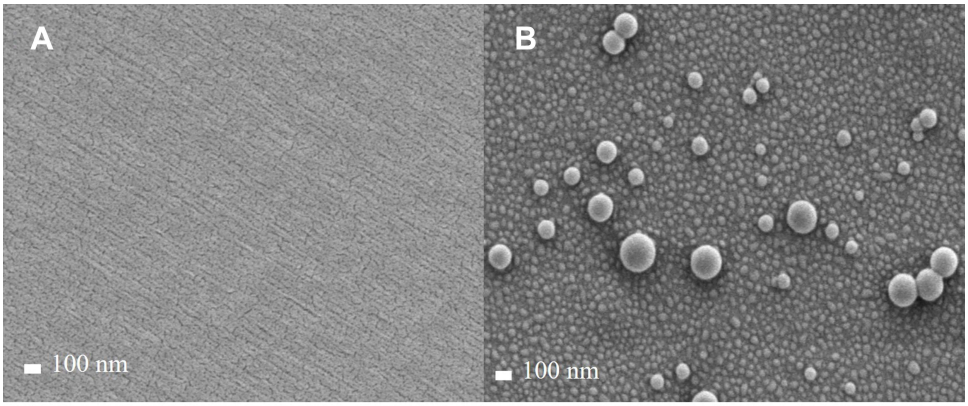

Figure 10 FE-SEM images of the PB-M surface (**A**), and 120 min after starting LON permeation (**B**).

Abbreviations

LEU, leuprolide; LEU acetate, leuprolide acetate; L18FCs, leuprolide-C18 fatty acid conjugates; LSC, leuprolide-stearic acid conjugate; LOC, leuprolide-oleic acid conjugate; LLC, leuprolide-linoleic acid conjugate; L18FNs, leuprolide-C18 fatty acid nanoparticles; LSN, leuprolide-stearic acid nanoparticle; LON, leuprolide-oleic acid nanoparticle; LLN, leuprolide-linoleic acid nanoparticle; NMR, nuclear magnetic resonance; MALDI-TOF, matrix-assisted laser desorption/ionization-time of flight; FT-IR, Fourier transform infrared spectroscopy; DSC, differential scanning calorimetry; DLS, dynamic light scattering; FE-SEM, field emission scanning electron microscope; FE-TEM, field emission transmission electron microscope; HPLC, high-performance liquid chromatography; Prep-HPLC, preparative-high-performance liquid chromatography; DW, deionized water; DMAP, 4-dimethylaminopyridine.

Data Sharing Statement

The data presented in this study are available upon request.

Acknowledgments

This work was primarily supported by a grant from the Korea Evaluation Institute of Industrial Technology (KEIT) funded by the Ministry of Trade, Industry and Energy, Republic of Korea (20008840) in 2020. We would like to thank the staff of the Ajou Central Laboratory for allowing us to use the FE-SEM, FE-TEM, DSC, and FT-IR facilities.

Disclosure

Kye Wan Lee reports grants from Ministry of Trade, Industry & Energy (MOTIE, Korea), during the conduct of the study, and is an employee of Dongkook Pharmaceutical Co., Ltd, Seoul, Republic of Korea. The authors report no other potential conflicts of interest in relation to this work and declare that they have no known competing financial interests or personal relationships that could have influenced the work reported in this paper.

References

1. Jagot-Lacoussiere L, Kotula E, Villoutreix BO, Bruzzoni-Giovanelli H, Poyet JL. A cell-penetrating peptide targeting AAC-11 specifically induces cancer cells death. *Cancer Res*. 2016;76(18):5479–5490. doi:10.1158/0008-5472.can-16-0302
2. Usmani SS, Bedi G, Samuel JS, et al. THPdb: database of FDA-approved peptide and protein therapeutics. *PLoS One*. 2017;12(7):e0181748. doi:10.1371/journal.pone.0181748
3. Lau JL, Dunn MK. Therapeutic peptides: historical perspectives, current development trends, and future directions. *Bioorg Med Chem*. 2018;26(10):2700–2707. doi:10.1016/j.bmc.2017.06.052
4. Cook T, Sheridan WP. Development of GnRH antagonists for prostate cancer: new approaches to treatment. *Oncologist*. 2000;5(2):162–168. doi:10.1634/theoncologist.5-2-162
5. Plosker GL, Brogden RN. Leuprorelin. A review of its pharmacology and therapeutic use in prostatic cancer, endometriosis and other sex hormone-related disorders. *Drugs*. 1994;48(6):930–967. doi:10.2165/00003495-199448060-00008

6. Rosario DJ, Davey P, Green J, et al. The role of gonadotrophin-releasing hormone antagonists in the treatment of patients with advanced hormone-dependent prostate cancer in the UK. *World J Urol*. 2016;34(12):1601–1609. doi:10.1007/s00345-016-1818-2
7. Luan X, Bodmeier R. In situ forming microparticle system for controlled delivery of leuprolide acetate: influence of the formulation and processing parameters. *Eur J Pharm Sci*. 2006;27(2–3):143–149. doi:10.1016/j.ejps.2005.09.002
8. Gallagher JS, Missmer SA, Hornstein MD, Laufer MR, Gordon CM, DiVasta AD. Long-term effects of gonadotropin-releasing hormone agonists and add-back in adolescent endometriosis. *J Pediatr Adolesc Gynecol*. 2018;31(4):376–381. doi:10.1016/j.jpag.2018.03.004
9. Morales JO, Huang S, Williams RO 3rd, McConville JT. Films loaded with insulin-coated nanoparticles (ICNP) as potential platforms for peptide buccal delivery. *Colloids Surf B Biointerfaces*. 2014;122:38–45. doi:10.1016/j.colsurfb.2014.05.025
10. Nguyen OOT, Tran KD, Ha NT, Doan SM, Dinh TTH, Tran TH. Oral cavity: an open horizon for nanopharmaceuticals. *J Pharm Invest*. 2021;51(4):413–424. doi:10.1007/s40005-021-00530-2
11. Kim Y-C, Min KA, Jang D-J, et al. Practical approaches on the long-acting injections. *J Pharm Invest*. 2020;50(2):147–157. doi:10.1007/s40005-019-00452-0
12. Zheng Y, Qiu Y, Lu MF, Hoffman D, Reiland TL. Permeability and absorption of leuprolide from various intestinal regions in rabbits and rats. *Int J Pharm*. 1999;185(1):83–92. doi:10.1016/S0378-5173(99)00146-5
13. Haggag YA, Donia AA, Osman MA, El-Gizawy SA. Peptides as drug candidates: limitations and recent development perspectives. *Biomed J*. 2018;1:3.
14. Haviy F, Fitzpatrick TD, Nichols CJ, et al. Stabilization of the N-terminal residues of luteinizing hormone-releasing hormone agonists and the effect on pharmacokinetics. *J Med Chem*. 1992;35(21):3890–3894. doi:10.1021/jm00099a017
15. Ochi M, Wan B, Bao Q, Burgess DJ. Influence of PLGA molecular weight distribution on leuprolide release from microspheres. *Int J Pharm*. 2021;599:120450. doi:10.1016/j.ijpharm.2021.120450
16. Sophocleous AM, Desai KG, Mazzara JM, et al. The nature of peptide interactions with acid end-group PLGAs and facile aqueous-based microencapsulation of therapeutic peptides. *J Control Release*. 2013;172(3):662–670. doi:10.1016/j.jconrel.2013.08.295
17. Fu M, Zhuang X, Zhang T, Guan Y, Meng Q, Zhang Y. PEGylated leuprolide with improved pharmacokinetic properties. *Bioorg Med Chem*. 2020;28(4):115306. doi:10.1016/j.bmc.2020.115306
18. Zhang F, Liu MR, Wan HT. Discussion about several potential drawbacks of PEGylated therapeutic proteins. *Biol Pharm Bull*. 2014;37(3):335–339. doi:10.1248/bpb.b13-00661
19. Han FY, Thurecht KJ, Whittaker AK, Smith MT. Bioerodable PLGA-based microparticles for producing sustained-release drug formulations and strategies for improving drug loading. *Front Pharmacol*. 2016;7:185. doi:10.3389/fphar.2016.00185
20. Kim D, Park C, Meghani NM, et al. Utilization of a fattigation platform gelatin-oleic acid sodium salt conjugate as a novel solubilizing adjuvant for poorly water-soluble drugs via self-assembly and nanonization. *Int J Pharm*. 2020;575:118892. doi:10.1016/j.ijpharm.2019.118892
21. Park C, Meghani N, Amin H, et al. The roles of short and long chain fatty acids on physicochemical properties and improved cancer targeting of albumin-based fattigation-platform nanoparticles containing doxorubicin. *Int J Pharm*. 2019;564:124–135. doi:10.1016/j.ijpharm.2019.04.038
22. Amin HH, Meghani NM, Oh KT, Choi H, Lee B-J. A conjugation of stearic acid to apotransferrin, fattigation-platform, as a core to form self-assembled nanoparticles: encapsulation of a hydrophobic paclitaxel and receptor-driven cancer targeting. *J Drug Deliv Sci Technol*. 2017;41:222–230. doi:10.1016/j.jddst.2017.07.013
23. Park C, Baek N, Loebenberg R, Lee BJ. Importance of the fatty acid chain length on in vitro and in vivo anticancer activity of fattigation-platform albumin nanoparticles in human colorectal cancer xenograft mice model. *J Control Release*. 2020;324:55–68. doi:10.1016/j.jconrel.2020.05.001
24. Kanikkannan N, Kandimalla K, Lamba SS, Singh M. Structure-activity relationship of chemical penetration enhancers in transdermal drug delivery. *Curr Med Chem*. 2000;7(6):593–608. doi:10.2174/0929867003374840
25. Dhimitruka I, Santalucia J Jr. Investigation of the Yamaguchi esterification mechanism. Synthesis of a lux-s enzyme inhibitor using an improved esterification method. *Org Lett*. 2006;8(1):47–50. doi:10.1021/ol0524048
26. Bech EM, Pedersen SL, Jensen KJ. Chemical strategies for half-life extension of biopharmaceuticals: lipidation and its alternatives. *ACS Med Chem Lett*. 2018;9(7):577–580. doi:10.1021/acsmedchemlett.8b00226
27. Eskandari S, Guerin T, Toth I, Stephenson RJ. Recent advances in self-assembled peptides: implications for targeted drug delivery and vaccine engineering. *Adv Drug Deliv Rev*. 2017;110–111:169–187. doi:10.1016/j.addr.2016.06.013
28. Pérez-López A, Martín-Sabroso C, Torres-Suárez AI. Timeline of translational formulation technologies for cancer therapy: successes, failures, and lessons learned therefrom. *Pharmaceutics*. 2020;12(11). doi:10.3390/pharmaceutics12111028
29. Meghani NM, Amin HH, Park C, et al. Design and evaluation of clickable gelatin-oleic nanoparticles using fattigation-platform for cancer therapy. *Int J Pharm*. 2018;545(1–2):101–112. doi:10.1016/j.ijpharm.2018.04.047
30. Satapathy SR, Sahoo RN, Satapathy B, Immani R, Panigrahi L, Mallick S. Development and characterization of leuprolide acetate encapsulated PLGA microspheres for parenteral controlled release depot injection. *Indian J Pharm Edu Res*. 2021;55(1):107–116. doi:10.5530/ijper.55.1.14
31. Cao SJ, Xu S, Wang HM, et al. Nanoparticles: oral delivery for protein and peptide drugs. *AAPS PharmSciTech*. 2019;20(5):190. doi:10.1208/s12249-019-1325-z
32. Kim H, Song D, Ngo HV, et al. Modulation of the clinically accessible gelation time using glucono-d-lactone and pyridoxal 5'-phosphate for long-acting alginate in situ forming gel injectable. *Carbohydr Polym*. 2021;272:118453. doi:10.1016/j.carbpol.2021.118453
33. Hac-Wydro K, Wydro P. The influence of fatty acids on model cholesterol/phospholipid membranes. *Chem Phys Lipids*. 2007;150(1):66–81. doi:10.1016/j.chemphyslip.2007.06.213
34. Padula C, Pescina S, Nicoli S, Santi P. New insights on the mechanism of fatty acids as buccal permeation enhancers. *Pharmaceutics*. 2018;10(4). doi:10.3390/pharmaceutics10040201
35. Ghasemiyeh P, Mohammadi-Samani S. Potential of nanoparticles as permeation enhancers and targeted delivery options for skin: advantages and disadvantages. *Drug Design Develop Ther*. 2020;14:3271–3289. doi:10.2147/dddt.s264648